Numerical and Experimental Investigation of Acetic Acid Decomposition by a Nano-Pulse Discharged Bubble in Water

Y. He, S. Uehara, H. Takana, and H. Nishiyama
Institute of Fluid Science, Tohoku University, Japan

Abstract—Nano-pulse discharges in bubbles are regarded as an efficient method to generate plasma for decomposition of persistent organic pollutants (POPs) in water. In this study, decomposition experiments of acetic acid solution by multiple nano-pulse discharged bubbles were firstly conducted for different voltages and frequencies under the same input power. It is found that the concentration of acetic acid solution decreased most for lower applied voltage and higher frequency. Moreover, a two-dimensional r-θ numerical model was constructed to investigate the decomposition characteristics of acetic acid by a nano-pulse discharged bubble. Hydroxyl radicals ($\cdot$OH) with high oxidation potential were generated in bubbles to decompose POPs. They were found to be able to diffuse through the bubble interface to several micrometers in water. The results showed that acetic acid were decomposed by OH radicals. The average decomposition rate was dependent on the water layer thickness. It is also found that for a given input power, acetic acid were mostly decomposed for lower applied voltage and higher frequency. The numerical results showed qualitative consistency with the experimental results.

Keywords—Water treatment, nano-pulse discharged bubble, hydroxyl radicals, acetic acid decomposition

I. INTRODUCTION

Although access to safe drinking water has been improved over the last decades, approximately one billion people still lack access to safe water and over 2.5 billion lack access to adequate sanitation. The health effects of water pollution have been an important research topic in environmental science, epidemiology, environmental economics, and health economics for centuries [1], [2]. Persistent organic pollutants (POPs), used as pesticides, solvents and pharmaceuticals currently or in the past, are considered to have the potential adverse impacts on human health and the environment because they are resistant to environmental degradation through chemical, biological and photolytic processes [3]. Due to their persistence in the environment, it may take them decennia or centuries to be degraded. Therefore, POPs released in water will easily enter the food-chain and eventually result in health problems not only among human beings but also among animals [4], [5].

Recent years, technologies for degradation of POPs have been rapidly developed. Advanced oxidation processes (AOPs) are considered as a promising remediation technology for water treatment by using hydroxyl radicals ($\cdot$OH) which has extremely high oxidation potential to decompose POPs in water [6], [7]. However, since the lifetime of the OH radical is rather short, they need to be generated and react with other pollutants simultaneously in water or near the water surface.

So far, various discharge methods for generating plasmas have been studied extensively. Takeuchi et al. [8] has developed experiment that generates gas phase plasmas between metal needles and a metal electrode in water. Magureanu et al. [9] has proposed a plasma reactor in which the pentoxifylline solution was circulated by a peristaltic pump and was made a flow as a film near a gas phase plasma. This reactor shows a relatively high removal efficiency of pentoxifylline. Direct discharges in liquid phase can generate OH radicals that can react with POPs immediately after being generated. However, it requires a rapid breakdown process driven by strong reduced electric field (E/N) [10], [11]. That causes a higher energy consumption for the decomposition of POPs. Nishiyama et al. [12], [13] constructed an innovative multiple bubble jet system to generate plasma in bubbles for water treatment. The generation of OH radicals, decolorization characteristics of methylene blue solution as well as decomposition of acetic acid were confirmed by these research works. This method requires less energy to initiate the discharge compared with other methods since the discharge occurs in the gases inside bubbles. Another excellence is that OH radicals can be utilized for reactions with pollutants simultaneously upon generation.

In order to improve the reactor designs for higher degradation efficiency of POPs, it is necessary to investigate the mechanisms of the plasmas generations and their diffusions around the plasma-liquid interfaces. Since it is difficult to measure the number density of OH radicals in the experiment due to its short lifetime, numerical simulations of plasmas are useful. Kushner et al. [14], [15] has established pioneering and landmark works on the investigation of electric discharge streamer propagation of gaseous bubbles immersed in liquids. A zero-dimensional numerical simulation was carried out by Matsui et al. to analyze the radical generation processes in the gas phase and decomposition of acetic acid in the liquid phase by a discharged bubble [16].

Our group has constructed a zero-dimensional model to study the chemical reactions in a nano-pulse discharged bubble [17]. The optimum conditions such as initial gas composition, applied voltage and frequency for the generation of OH radicals were obtained. Then, a two-dimensional numerical model for a discharged bubble was constructed by our group to investigate the diffusion processes of chemical species from the inside of a bubble to the liquid phase through the bubble interface when the streamer propagating along the bubble inner interface [18]. It was shown that OH radicals can diffuse

---

Corresponding author: Hideya Nishiyama
e-mail address: nishiyama@tohoku.ac.jp

several micrometers away from the bubble interface in liquid.

In this study, decomposition experiment of acetic acid by using a multiple bubble jets system with nanosecond pulsed discharge was carried out firstly. An improved cylindrical mesh electrode was utilized in this experiment for higher decomposition efficiency [19]. Then, numerical simulations based on a two-dimensional model were conducted to investigate the decomposition processes of acetic acid by OH radicals in the liquid phase. Lastly, a qualitative comparison between the numerical and experimental results is carried out to obtain the optimal operating conditions for decomposition of acetic acid in liquid.

II. EXPERIMENTAL ANALYSIS

A. *Experimental setup*

Fig. 1 shows the schematic illustration of a multiple bubble jets system for water treatment [13]. The experimental setup was described in detail in former studies and will only be briefly introduced here [13], [18]. This system consists of a nanosecond pulse power source (TE-HPS15K-A (C), Tamaoki Electronics), a water treatment reactor, electrodes and a gas feeding tube. There are five holes in a line along both the opposite tube side walls to generate multiple gas bubbles. Typical bubble sizes are ranged from 1 to 3 mm for stable discharge. The behavior of an ejected single bubble as well as the streamer discharge characteristics have been clarified in former research work [13].

A grounded cathode is placed in the center of the gas feeding tube and a cylindrical mesh anode is placed surrounding the bubble jets to generate discharge inside bubbles. It is reported that the decomposed concentration of acetic acid when using a cylindrical mesh anode is nearly twice as much as using a plate electrode which was placed at the bottom of the reactor [19]. The flow rate of feeding Ar gas is 3.0 Sl/min. The volume of acetic acid solution is 550 mL with the typical initial concentration of 170 mg/L. An ion chromatograph (Prominence HIC-NS, Shimadzu) is used to determine the concentration of ion species such as CH_3COO^- and $HCOO^-$ during the decomposition processes. The used column is Shim-Pack IC-A3 with a flow rate of 1.2 ml/min, which is a general-purpose column for inorganic anion and organic acid ion analysis. In the chromatograph, CH_3COOH concentrations as well as byproducts concentrations such as formic acid in the aqueous solution can be measured. The applied pulse voltages and frequencies are 5–9 kV and 500–2000 Hz, respectively. A typical waveform when applying 9 kV and 1000 Hz voltage is shown in Fig. 2. Waveforms from -200 ns to 1000 ns are shown in figure. The voltage rises to 9 kV within 75 ns and drops to 0 within 300 ns. Compared with the waveforms when using a plate electrode where the current rises to 6 A, the maximum current here is up to 28 A due to the uniform distance between anode and cathode which has increases the electric field strength in bubbles.

B. *Experimental results*

Fig. 3 shows the time evolutions of acetic acid concentrations during the decomposition processes for different voltages and frequencies with a fixed input power. The concentrations of acetic acid are measured by ion chromatography. Decomposition experiment of acetic acid is conducted under the Ar gas flow rate of 3.0 Sl/min. The consumed energies per pulse at different applied voltages are shown in Table I. According to Eq. (1), the corresponding frequencies for different voltages can be obtained when the input power is set to be 600 mW. For voltages below 5 kV voltage, discharges in bubbles cannot be sustained. Therefore, the lowest applied voltage is set to be 5 kV. The decomposition efficiencies of acetic acid are compared under different working conditions. The initial acetic acid solution volume is 550 mL and the solution concentration is 170 mg/l. Due to the measurement and solution preparation errors, the acetic acid solution concentrations are not exactly same at the initial state. The initial concentrations are around 170 mg/l and the little differences are supposed to have no effects on the decomposition rates.

It is reported that the CH_3COOH molecules can be decomposed only by OH radicals not by O radicals and active oxygen species O_3 since OH radicals have sufficiently high oxidation potential (2.80 V) than that of O (2.42 V) and O_3 (2.07)

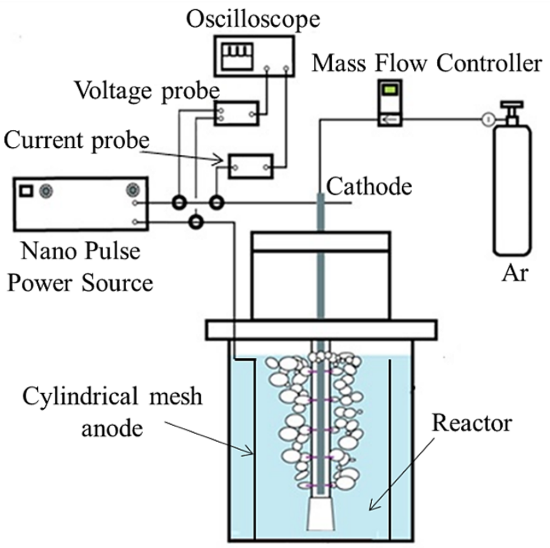

Fig. 1. Schematic illustration of multiple discharged Ar bubble jets.

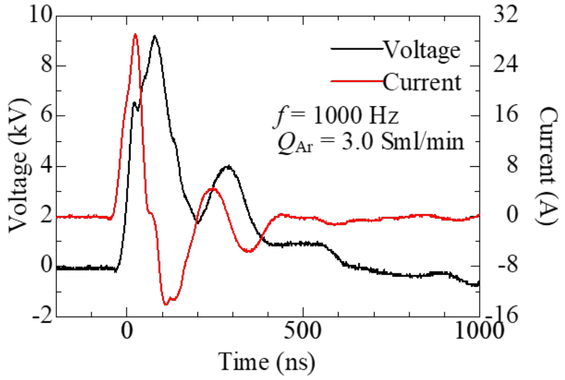

Fig. 2. Discharge characteristics for one pulse at V = 9 kV, f = 1000 Hz, and Q_{Ar} = 3.0 Sl/min.

TABLE I

CONSUMED ENERGIES PER PULSE FOR DIFFERENT VOLTAGES AND THE CORRESPONDING FREQUENCIES FOR A GIVEN INPUT POWER

Voltage	Energy per pulse $E_{\mathrm{int/pulse}}$ (mJ/pulse)	Frequency (Hz) (P = 600 mW)
5 kV	0.3	2000
7 kV	0.73	822
9 kV	1.297	462

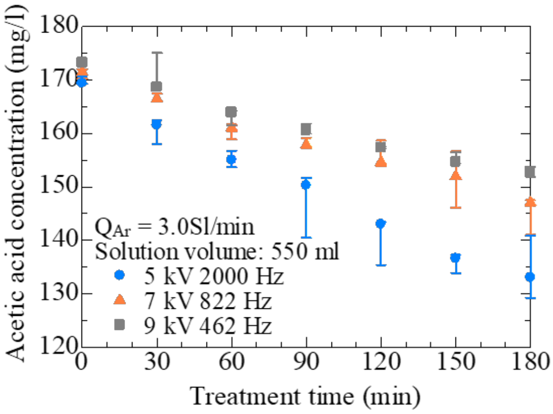

Fig. 3. Time evolutions of acetic acid concentrations under different applied voltages and frequencies.

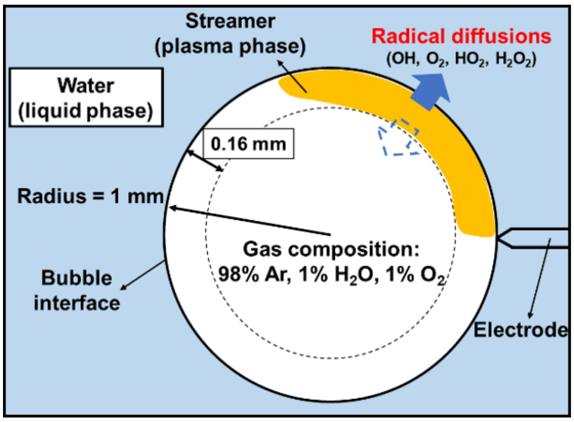

Fig. 4. Schematic illustration of a two-dimensional discharged bubble model.

radicals [20], [21]. OH radicals are generated by electron impact reaction (2) with water molecules in bubble or at bubble interface. For OH radicals generated in bubble, they diffuse to the solution through the bubble interface simultaneously and react with CH_3COOH molecules. Acetic acid are eventually decomposed to H_2O and CO_2 by OH radicals during the following processes [22].

$$P_{\mathrm{set}} = f \times E_{\mathrm{int/pulse}} \tag{1}$$

$$\mathrm{H_2O}_{\ (\mathrm{gas})} + \mathrm{e} \longrightarrow \cdot\mathrm{OH}_{\ (\mathrm{gas})} + \mathrm{H} + \mathrm{e} \tag{2}$$

$$\cdot\mathrm{OH}_{\ (\mathrm{gas})} \longrightarrow \cdot\mathrm{OH}_{\ (\mathrm{aq})} \tag{3}$$

$$\mathrm{CH_3COOH} + \cdot\mathrm{OH}_{\ (\mathrm{aq})} \longrightarrow \cdot\mathrm{CH_3COO} + \mathrm{H_2O} \tag{4}$$

$$\longrightarrow \mathrm{CO_2} + \cdot\mathrm{CH_3} + \mathrm{H_2O} \tag{5}$$

As shown in Fig. 3, acetic acid concentrations have apparently decreased after 180 min treatment by using discharged bubble jets. It is shown that, under the same input power, the acetic acid is decomposed more with 5 kV (2000 Hz) among the condition tested using the same input power. This result indicates that the optimal working condition for acetic acid decomposition is lower applied voltage and higher applied frequency under the same input power. This result agrees well with our former research work [18], in which OH radicals are found to be most generated for lower applied voltage and higher frequency, since OH radicals are considered to be the main factor for acetic acid decomposition.

III. NUMERICAL ANALYSIS

A. Description of the numerical model

A two-dimensional model of a nanosecond pulse discharged bubble which consists of a plasma phase inside the bubble and a liquid phase outside the bubble is constructed. The geometry of this numerical model was described in detail in our former studies and will be only briefly described here [17], [18].

Fig. 4 shows the schematic illustration of the two-dimensional r-θ numerical model. The radius of the bubble is 1 mm and the initial gas composition inside the bubble is Ar, O_2 and H_2O with a ratio of 0.98: 0.01: 0.01. During the 60 seconds, the bubble is considered to be continuously generated from the small hole of the gas feeding tube in the experiment which was explained in Sec. II.A. Therefore, the distortion or deformation of the bubble in microsecond scale are considered to have little effect on the diffusions from bubble to liquid thus the bubble is assumed to be non-deformable as an ideal condition. Consequently, the pressure inside the bubble in considered to be constant during the radical diffusions and chemical reactions processes. For a similar reason, the temperature inside the bubble is also considered to be stable at room temperature though we acknowledge that joule heating can occur in the bubble when discharge occurs and the temperature will increase rapidly up to 1000K in nanosecond scale [15].

Electrode is assumed to be positioned on the right side of the bubble, as shown in Fig. 4, with the angle set to be 0 degree in this model. The angle is assumed to increase in counterclockwise direction around the bubble. A streamer propagation with an average width of 0.16 mm is simulated from 0 to 180 degree along the upper bubble interface based on experimental visualization results that the streamer tended to head in one direction either on the upper or lower side along the bubble interface due to the different dielectric constants of gas and water [13]. The streamer head velocity is also obtained from experiment, which was estimated to be 3×10^6 cm/s by using an ultra-sensitive high-speed camera. In one pulse discharge of 500 μs for 2000 Hz frequency, the streamer head is assumed to propagate from 0 degree to 180 degree within approximately 104 ns and then stop at 180 degree until 500 μs as an ideal condition. Then it propagates from 0 degree again in the next pulse. The exited chemical species are considered to remain in the region of the former streamer.

Usually there is a higher reduced electric field E/N at the streamer head as conductive plasma forms in a bubble. However, E/N is assumed to be uniform in the streamer during streamer propagation since the present study focuses on species diffusions from bubble to liquid through the bubble interface and the chemical reactions in liquid. As a result, the species densities are uniform in the streamer and change only over time. A local simulation is utilized for calculating plasma chemical reactions dominated by E/N in the streamer [17]. The diffusions of chemical species from the streamer to liquid occur all the time in this simulation.

The governing equations in plasma phase, bubble interface as well as liquid phase are explained in [18] in detail so will be only listed here. The diffusions of chemical species from bubble to liquid at the bubble interface are governed by Henry's law and the liquid phase diffusions are dominated by Fick's law.

$$\frac{\partial C_{p,s}}{\partial t} = G_{p,s} - L_{p,s} \tag{6}$$

$$\frac{\partial C_{l,s}}{\partial t} = G_{l,s} - L_{l,s} + D_l \left\{ \frac{1}{r}\frac{\partial}{\partial r}\left(r\frac{\partial C_{l,s}}{\partial r} \right) + \frac{1}{r^2}\frac{\partial^2 C_{l,s}}{\partial \theta^2} \right\} \tag{7}$$

$$F_{\text{in}} = D_{pl,s}\frac{C_{p,s} - C_{l,s}}{\Delta r} \tag{8}$$

$$D_{pl,s} = D_{p,s}\left(\frac{h_s C_{p,s} - C_{l,s}}{h_s C_{p,s}} \right) \tag{9}$$

where $C_{p,s}$, $C_{l,s}$ refer to the species concentrations in plasma phase and liquid phase, respectively. $G_{p,s}$, $G_{l,s}$ refer to the generated concentrations of species in plasma phase and liquid phase, respectively. D_l, $D_{pl,s}$, $D_{p,s}$ are diffusion coefficients of each species in liquid phase, plasma-liquid interface and plasma phase. F_{in} refers to the diffusion flux from plasma phase to liquid phase through bubble interface. h_s is Henry's law constant, which is different for different chemical species [18].

Different from the former model [18], chemical reaction between OH radicals and acetic acid in liquid phase is introduced in this study. Although it has been suggested that acetic acid is decomposed by a complex process and by-products such as formic acid and oxalic acid will be generated [21], the decomposition reactions are simplified to be one dominant reaction in this model [23]. All the liquid phase reactions are listed in Table II. Four kinds of reactive oxygen species (ROS) as well as CH_3COOH are considered in the liquid phase. The diffusion coefficients in a liquid for all chemical species are given to be 1×10^{-1} m^2/s due to the lack of chemical database [24].

B. Numerical results

Fig. 5 shows the OH and CH_3COOH distributions in liquid after 60 seconds for acetic acid decomposition. The operating conditions are V = 5 kV, f = 2000 Hz. According to Table I, the input energy per pulse is 0.3 mJ. The mesh size for the entire computational region is 0.1 μm, which was previously proved to be a reasonable value for both accurate calculation and less CPU time [18]. The initial acetic acid concentration in liquid is 0.0001 mol/l for all cases. The water layer thickness in numerical simulations are set as 10 μm, 20 μm and 30 μm, respectively. 0 μm in the horizontal axis represents the bubble interface. From the previous research, there was almost no difference of OH concentrations in the circumferential direction around the bubble interface in liquid after 500 μs [18]. This is because that compared with one pulse discharge time of 500 μs, the streamer propagation time of 104 ns from 0 to 180 degree is comparably small. As a result, the streamer is constant at 180 degree in most of the calculation time so that the diffusion from the inside bubble liquid occurs uniformly from 0 to 180 degree. Therefore, only the results in 90 degree direction from the bubble interface to liquid are shown in this figure.

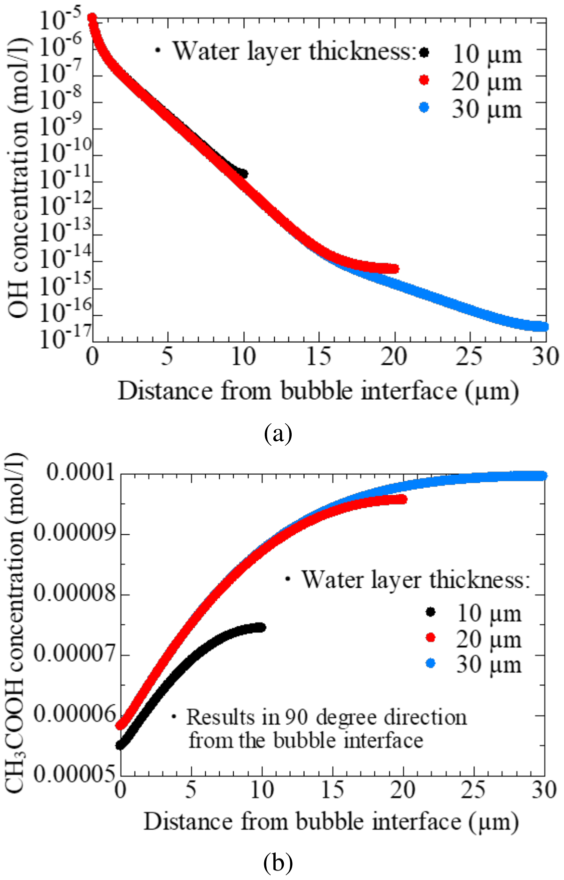

(a)

(b)

Fig. 5. Distributions of (a) OH radicals and (b) CH_3COOH in liquid for different water layer thicknesses.

Fig. 5 (a) shows that for the same region in liquid phase, the OH concentrations are nearly not dependent on the water layer thickness. However, CH_3COOH in the same region in liquid (for example, 0–10 μm region) has higher concentration for water layer thicknesses of 30 μm than that for 10 μm, as shown in Fig. 5 (b).

This is resulted from the CH_3COOH diffusions from area

TABLE II
LIQUID PHASE REACTIONS

No.	Reaction	Rate coefficient ($m^3/(mol \cdot s)$)	Ref.
1	$OH + OH \longrightarrow H_2O_2$	4.0×10^6	[8]
2	$OH + HO_2 \longrightarrow H_2O + O_2$	$7.0 \times 10^6 \exp(-1700/T_{liq})$	[25]
3	$OH + H_2O_2 \longrightarrow HO_2 + H_2O$	$2.7 \times 10^4 \exp(-1500/T_{liq})$	[25]
4	$2\,HO_2 \longrightarrow H_2O_2 + O_2$	$8.6 \times 10^2 \exp(-2365/T_{liq})$	[25]
5	$H_2O_2 + HO_2 \longrightarrow OH + H_2O + O_2$	5.0×10^{-4}	[25]
6	$OH + CH_3COOH \longrightarrow CH_3 + CO_2 + H_2O$	1.6×10^4	[26]

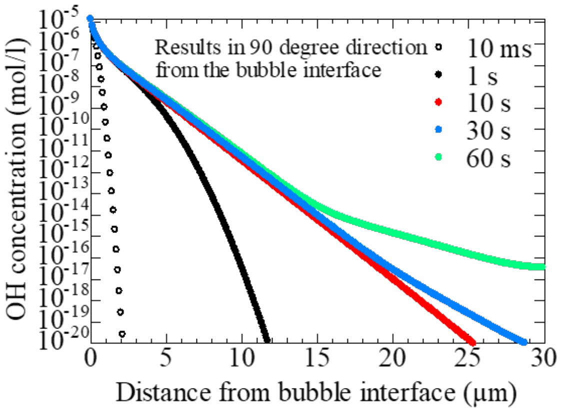

Fig. 6. OH distributions in 90 degree direction from the bubble interface to liquid during 60 seconds simulation.

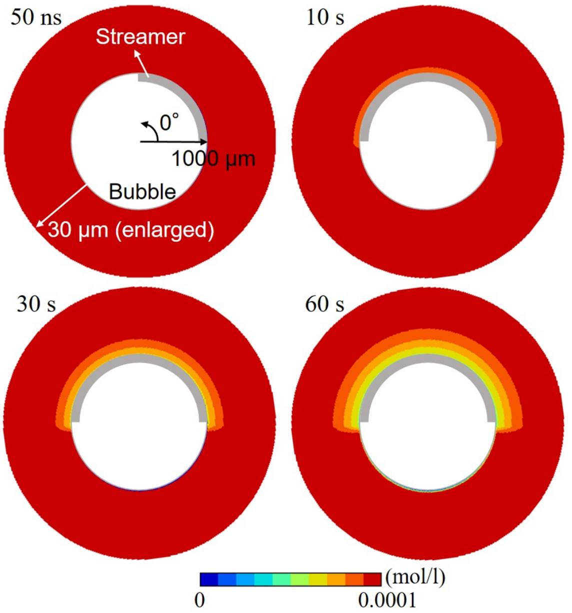

Fig. 7. CH_3COOH distributions in liquid phase during 60 second treatment when the initial concentration of 0.0001 mol/l.

away from the bubble interface (where acetic acid are less or nearly not decomposed) to area near bubble interface where CH_3COOH are much more decomposed by OH radicals. As a result, CH_3COOH concentrations near the bubble interface are higher for larger water layer thickness due to the larger CH_3COOH diffusions from area away from the bubble interface. Moreover, since CH_3COOH concentration keeps at the initial concentration at 30 μm, the water layer thickness of 30 μm is considered to be a reasonable value for this numerical simulation for acetic acid decomposition. Therefore, the following simulations are all conducted with a 30 μm water layer thickness.

Fig. 6 shows the OH distributions in 90 degree direction in liquid during 60 seconds. 0 μm represents the bubble interface and 30 μm represents the furthest position in the liquid phase. It is shown that OH concentration at 30 μm is about $1/10^{11}$ of that at bubble interface. The effect of diffusion gains for OH radicals in liquid phase are considered to be larger than that of the consumptions in chemical reactions with acetic acid since the OH concentrations in the liquid phase keep increasing during 60 seconds. Moreover, OH concentrations in 0–5 μm region do not change after 1 second. This indicates that the OH concentrations here has reached an equilibrium state between the chemical reactions and diffusions.

Fig. 7 shows the CH_3COOH concentration distributions in liquid during 60 seconds treatment. The initial concentration of CH_3COOH is 0.0001 mol/l uniformly in the liquid phase. It is found that in the first 10 seconds, acetic acid are almost not decomposed.

Then, CH_3COOH in the area near the bubble radicals which were diffused from the streamer. It is found CH_3COOH in this area have been decomposed by about 50% after 60 s. CH_3COOH within 15 μm from the bubble interface are decomposed and there is nearly no decomposition for CH_3COOH in 15–30 μm. Moreover, it can be found that CH_3COOH in the opposite side area of the streamer are nearly not decomposed. This is because that compared with the 2-D bubble circumference of 0.628 cm in θ-direction, the liquid region shown in the figure has been enlarged and it is only 30 μm in r-direction. Therefore, OH radicals can almost not diffuse in θ-direction.

Fig. 8 shows the effect of initial CH_3COOH concentration on decomposition in the liquid phase. Initial concentrations of 1×10^{-2} mol/l, 1×10^{-3} mol/l and 1×10^{-4} mol/l are given. The decomposition rates for all positions in liquid in 90 degree direction from the bubble interface are shown in figure. It shows that the decomposition rate is higher for lower initial concentration near the bubble interface and the decomposition rates are approximately 42%, 40% and 36% for three cases after 60 seconds. It can be also found that the decomposition rates gradually decrease by distance from the bubble interface and become nearly the same for all cases at larger than 20 μm.

TABLE III

A QUALITATIVE COMPARISON BETWEEN THE NUMERICAL AND EXPERIMENTAL RESULTS FOR DIFFERENT CONDITIONS

Conditions	Decomposed CH_3COOH after 3 h (Experiment)	Volume integral of CH_3COOH decomposition rates (Simulation)
5 kV, 2000 Hz	1.77	1.84
7 kV, 822 Hz	1.19	1.29
9 kV, 462 Hz	1	1

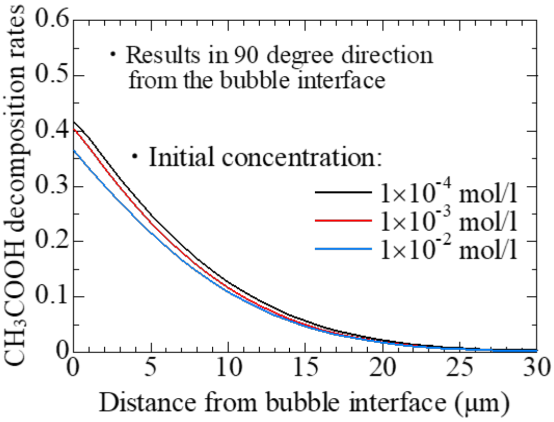

Fig. 8. Distributions of CH_3COOH in liquid phase for various initial concentrations.

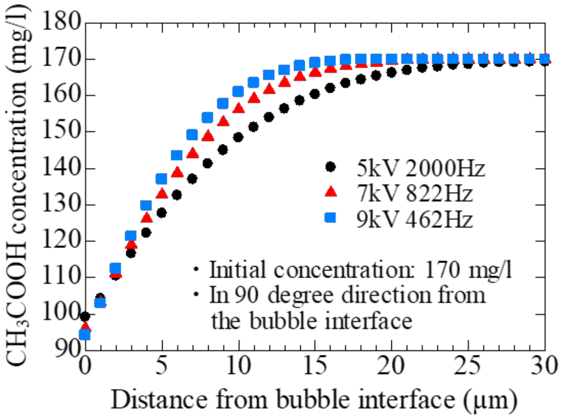

Fig. 9. Distributions of CH_3COOH in liquid phase for different applied voltages and frequencies for bubble discharge.

On the other hand, compared with the decomposition rates of about 20% after 3 hours in experiment which was introduced in Sec. II.B, the decomposition rates in numerical simulation are apparently higher. This is affected by the neglected energy loss in simulations as well as the neglected by-products generations such as formic acid and oxalic acid during the decomposition processes. The total consumed energy for the experimental system is utilized in the numerical simulations and all the energy are applied only on the discharges in a bubble. However, the total consumed energy has not been completely utilized only for bubble discharges in the experiment due to the energy losses for joule heating in solution. Therefore, it is reasonable that the decomposition rate in numerical simulation is much higher than experiment.

C. Comparison with experimental results

Fig. 9 investigates the effect of applied voltage and frequency on CH_3COOH decompositions in liquid. In accordance to the working conditions in experiment, the applied voltages and frequencies are set to 5 kV (2000 Hz), 7 kV (822 Hz) and 9 kV (462 Hz) for a same input power. The initial concentration is 2.831 mol/l, refers to 170 mg/l which is used for experimental study as well. The distributions of CH_3COOH in 90 degree direction from bubble interface are shown in figure. It is apparent that CH_3COOH are more decomposed for lower applied voltages and higher frequencies since OH radicals are more generated in these conditions [18]. However, the decomposition rates in the numerical simulation are still much larger than experimental results. As explained before, this is resulted from the neglected energy losses and by-products generations in numerical simulations.

Table III shows a qualitative comparison between the numerical and experimental results for different applied voltages and frequencies under the same input power. For the numerical results, the volume integrals in Fig. 9 are calculated to obtain the average decomposition rates of CH_3COOH in the liquid phase. On the other hand, since the average concentration of the acetic acid solution can be obtained from ion chromatograph, the average CH_3COOH decomposition rates of the solutions after 3 hours treatments are used. The results for 9 kV (462 Hz) are normalized for numerical simulation and experiment, respectively. It is found that CH_3COOH are most decomposed for 5 kV (2000 Hz). Although more OH radicals can diffuse to liquid phase to decompose CH_3COOH for 9 kV (462 Hz) in a single discharge pulse, the diffusion amount of OH radicals in each pulse is relatively low. Therefore, more discharge pulses in a same time can realize more OH diffusion from the bubble to liquid phase. As a result, CH_3COOH can be more decomposed under 5 kV (2000 Hz) condition. Moreover, it shows a qualitatively good agreement between the numerical and the experimental results.

IV. CONCLUSIONS

In this study, a two-dimensional numerical model for a nano-pulse discharged bubble was constructed for the multiple bubble jets system. In order to improve the reactor designs of bubble discharges for higher degradation efficiency of persistent organic pollutants in practice, the decompositions of acetic acid by OH radicals both in numerical simulation and experiment are conducted. The obtained results are as follows.

1) For different computational domain with water layer thicknesses of 10 μm, 20 μm and 30 μm, OH concentrations in the same region (for example, 0–10 μm

region) are nearly same for all cases. However, the remaining CH_3COOH concentration in this region is higher for larger water layer thicknesses after 60 seconds of decomposition. This is due to the undecomposed CH_3COOH in area away from the bubble interface that diffuses into 0–10 μm region where lower CH_3COOH concentration by decomposition.

2) The average decomposition rates of CH_3COOH in the numerical simulations under the same condition are found to be much higher than that in the experiment. This difference comes from the neglected energy loss in a solution by joule heating in numerical simulation, as well as the neglected by-products generations such as formic acid and oxalic acid in the decomposition processes in numerical simulation.
3) What is important, the numerical result shows a qualitatively good agreement with experimental result that acetic acid can be more decomposed under the condition of a lower applied voltage and higher frequency for the same input power.

ACKNOWLEDGMENT

The present study was partially supported by JSPS KAKENHI Grant Number 26249015 in 2016-2018. We would like to give our thanks to Mr. T. Nakajima for his technical support.

REFERENCES

[1] I. A. Shiklomanov and J. C. Rodda, *World Water Resources at the Beginning of the Twenty-First Century*. Cambridge University Press, 2003.
[2] S. Kulshreshtha, "A global outlook for water resources to the year 2025," *Water Resources Management*, vol. 12, pp. 167–184, 1998.
[3] F. Wania and D. Mackay, "Tracking the distribution of persistent organic pollutants," *Environmental Science and Technology*, vol. 30, pp. 390A–397A, 1996.
[4] R. Weber, A. Watson, M. Forter, and F. Oliaei, "Persistent organic pollutants and landfills - a review of past experiences and future challenges," *Waste Management and Research*, vol. 29, pp. 107–121, 2011.
[5] R. A. Etzel, "Polychlorinated biphenyls, dibenzofurans and dibenzodioxins," in *Pediatric Environmental Health*, 2nd ed. American Academy of Pediatrics Committee on Environmental Health, 2003.
[6] J. O. Tijani, O. O. Fatoba, G. Madzivire, and L. F. Petrik, "A review of combined advanced oxidation technologies for the removal of organic pollutants from water," *Water, Air, and Soil Pollution*, vol. 225, p. 2102, 2014.
[7] M. Antonopoulou, E. Evgenidou, D. Lambropoulou, and I. Konstantinou, "A review on advanced oxidation processes for the removal of taste and odor compounds from aqueous media," *Water Research*, vol. 53, pp. 215–234, 2014.
[8] N. Takeuchi, M. Ando, and K. Yasuoka, "Investigation of the loss mechanisms of hydroxyl radicals in the decomposition of organic compounds using plasma generated over water," *Japanese Journal of Applied Physics*, vol. 54, p. 116201, 2015.
[9] M. Magureanu, D. Piroi, N. B. Mandache, and V. Parvulescu, "Decomposition of methylene blue in water using a dielectric barrier discharge: Optimization of the operating parameters," *Journal of Applied Physics*, vol. 104, p. 103306, 2008.
[10] P. J. Bruggeman, M. J. Kushner, B. R. Locke, J. G. E. Gardeniers, W. G. Graham, D. B. Graves, R. C. H. M. Hofman-Caris, D. Maric, J. P. Reid, E. Ceriani, D. Fernandez Rivas, J. E. Foster, S. C. Garrick, Y. Gorbanev, S. Hamaguchi, F. Iza, H. Jablonowski, E. Klimova, J. Kolb, F. Krcma, P. Lukes, Z. MacHala, I. Marinov, D. Mariotti, S. Mededovic Thagard, D. Minakata, E. C. Neyts, J. Pawlat, Z. L. Petrovic, R. Pflieger, S. Reuter, D. C. Schram, S. Schröter, M. Shiraiwa, B. Tarabová, P. Tsai, J. R. R. Verlet, T. Von Woedtke, K. R. Wilson, K. Yasui, and G. Zvereva, "Plasma-liquid interactions: A review and roadmap," *Plasma Sources Science and Technology*, vol. 25, p. 053002, 2016.
[11] K. Schoenbach, J. Kolb, S. Xiao, S. Katsuki, Y. Minamitani, and R. Joshi, "Electrical breakdown of water in microgaps," *Plasma Sources Science and Technology*, vol. 17, p. 024010, 2008.
[12] H. Nishiyama, R. Nagai, K. Niinuma, and H. Takana, "Characterization of DBD multiple bubble jets for methylene blue decolorization," *Journal of Fluid Science and Technology*, vol. 8, pp. 65–74, 2013.
[13] H. Nishiyama, K. Niinuma, S. Shinoki, and H. Takana, "Decomposition of acetic acid using multiple bubble jets with pulsed electrical discharge," *Plasma Chemistry and Plasma Processing*, vol. 35, pp. 339–354, 2015.
[14] N. Y. Babaeva and M. J. Kushner, "Structure of positive streamers inside gaseous bubbles immersed in liquids," *Journal of Physics D: Applied Physics*, vol. 42, p. 132003, 2009.
[15] W. Tian, K. Tachibana, and M. J. Kushner, "Plasmas sustained in bubbles in water: Optical emission and excitation mechanisms," *Journal of Physics D: Applied Physics*, vol. 47, p. 055202, 2014.
[16] Y. Matsui, N. Takeuchi, K. Sasaki, R. Hayashi, and K. Yasuoka, "Experimental and theoretical study of acetic-acid decomposition by a pulsed dielectric-barrier plasma in a gas-liquid two-phase flow," *Plasma Sources Science and Technology*, vol. 20, p. 034015, 2011.
[17] Y. He, S. Uehara, H. Takana, and H. Nishiyama, "Numerical modelling and simulation of chemical reactions in a nano-pulse discharged bubble for water treatment," *Plasma Science and Technology*, vol. 18, pp. 924–932, 2016.
[18] Y. He, S. Uehara, H. Takana, and H. Nishiyama, "Experimental and theoretical study on chemical reactions and species diffusion by a nano-pulse discharged bubble for water treatment," *European Physical Journal D*, vol. 72, p. 11, 2018.
[19] K. Ishihata and H. Nishiyama, "Decomposition of acetic acid using multiple bubble jets with nanosecond pulsed discharge," in *The 11th International Conference on Flow Dynamics*, 2014, pp. OS10–26.
[20] K. Sato, K. Yasuoka, and S. Ishii, "Water treatment with pulsed plasmas generated inside bubbles," *IEEJ Transactions on Fundamentals and Materials*, vol. 128, pp. 401–406, 2008.
[21] T. Shibata and H. Nishiyama, "Acetic acid decomposition in a coaxial dielectric barrier discharge tube with mist flow," *Plasma Chemistry and Plasma Processing*, vol. 34, pp. 1331–1343, 2014.
[22] Y.-W. Huang, T. J. Dransfield, J. D. Miller, R. D. Rojas, X. G. Castillo, and J. G. Anderson, "Experimental study of the kinetics of the reaction of acetic acid with hydroxyl radicals from 255 to 355 K," *Journal of Physical Chemistry A*, vol. 113, pp. 423–430, 2009.
[23] N. I. Butkovskaya, A. Kukui, N. Pouvesle, and G. Le Bras, "Rate constant and mechanism of the reaction of OH radicals with acetic acid in the temperature range of 229-300 K," *Journal of Physical Chemistry A*, vol. 108, pp. 7021–7026, 2004.
[24] E. L. Cussler, "Values of diffusion coefficients," in *Diffusion: Mass Transfer in Fluid Systems*, 3rd ed. Cambridge University Press, 2009, ch. 5, pp. 117–160.
[25] S. N. Pandis and J. H. Seinfeld, "Sensitivity analysis of a chemical mechanism for aqueous-phase atmospheric chemistry," *Journal of Geophysical Research*, vol. 94, pp. 1105–1126, 1989.
[26] N. Karpel Vel Leitner and M. Dore, "Hydroxyl radical induced decomposition of aliphatic acids in oxygenated and deoxygenated aqueous solutions," *Journal of Photochemistry and Photobiology A: Chemistry*, vol. 99, pp. 137–143, 1996.